Determination of nicotine in e-liquids by electrochemical generation of surface-enhanced Raman scattering substrates[☆]

Luis Romay , Martin Perez-Estebanez , Aranzazu Heras , Alvaro Colina [*]

Departamento de Química, Universidad de Burgos. Facultad de Ciencias, Plaza Misael Bañuelos, s/n E-09001, Burgos, España, Spain

ARTICLE INFO

ABSTRACT

Quantitative methods using surface-enhanced Raman scattering (SERS) for analysis in complex matrices are very attractive due to the high sensitivity and selectivity of this technique. In this work, a novel time-resolved electrochemical surface-enhanced Raman scattering (TR-EC-SERS) analytical method has been developed for the determination of nicotine in e-liquids of electronic cigarettes. One of the main challenges of SERS is its inherent lack of reproducibility. Here, this limitation was mitigated by employing an electrochemical pre-treatment step to generate a homogeneous distribution of silver nanoparticles (Ag-NPs) on a silver screen-printed electrode. The enhanced Raman scattering induced by the Ag-NPs enabled the detection of nicotine at nanomolar levels. The high sensitivity of the method allowed the quantitative analysis of diluted e-liquid samples, mitigating potential interferences from other components present in these complex matrices. Moreover, TR-EC-SERS, coupled with parallel factor analysis (PARAFAC), demonstrated the capability of trilinear spectroelectrochemistry data not only to detect nicotine but also to identify potential interfering compounds without prior knowledge of their spectral signatures. This multivariate approach offers significant potential for the detection of outliers in complex samples.

1. Introduction

Electronic cigarettes (e-cigarettes) are battery-powered electrical devices that use a coil to heat a liquid (e-liquid) to produce an aerosol which is inhaled by the user. These e-liquids consist of a mixture of propylene glycol (PG) and vegetable glycerine (VG) in varying proportions, combined with flavouring and colouring compounds [1,2]. Some e-cigarettes are nicotine-free, and others may contain nicotine in two different forms: while certain e-cigarettes contain nicotine in its free form, with a concentration between 1 and 18 mg/mL, others present it in the form of one of its salts, with a concentration between 1 and 50 mg/mL [3,4]. E-cigarettes have gained popularity in recent years as a method of smoking cessation, nevertheless, there is a growing concern about the increasing prevalence of e-cigarette use among the young non-smoking population [5–7].

Given the addictive and toxic nature of the nicotine present in e-liquids [1,8] and the discrepancies observed between the results of analyses and the nicotine content labelled in the samples [7], there has been a growing demand for a specific analysis for this substance in recent years. The most commonly employed methods for the determination of nicotine in e-liquids are based on chromatographic and mass spectroscopy techniques that are distinguished by their high accuracy [9–13]. Nevertheless, these techniques require complex sample handling and long analysis periods, rendering them unsuitable in a point of care analysis.

Nicotine analysis by surface-enhanced Raman scattering (SERS) has been proposed as an alternative that significantly helps to overcome the limitations of current used techniques. SERS is able to enhance the Raman scattering signal of many molecules by several orders of magnitude, due to the presence of nanoparticles (NPs) of noble metals such as gold, silver or copper, among others [14,15]. Previous studies have investigated the use of chemically synthesised gold or silver NPs dispersed on a surface to generate SERS substrates for the analysis of nicotine [16–22]. However, these methods have implicit disadvantages, such as the need for complex and time-consuming synthesis of plasmonic NPs prior to the measurement.

Time-resolved electrochemical surface-enhanced Raman spectroscopy (TR-EC-SERS) [23] is presented as an alternative to avoid all the

aforementioned drawbacks. The use of electrochemistry enables the electrosynthesis of SERS substrates on the surface of silver, gold or copper electrodes [24–26] in a reproducible and simple way. The combination of electrochemistry and Raman spectroscopy in TR-EC-SERS experiments allows the *operando* performance evaluation of the electrogenerated SERS substrate, providing valuable and correlated information from two different points of view for the rational design of analytical methodologies. Moreover, TR-EC-SERS provides a three-way array of spectroelectrochemistry data which can be analysed using multivariate statistical tools to extract much more reliable information on the studied system respect to a simple univariate analysis. For the aforementioned reasons, the use of TR-EC-SERS has emerged in the past years as an attractive alternative to improve the reproducibility of SERS methodologies, especially when using screen-printed electrodes (SPEs) [27,28].

In this work, the use of TR-EC-SERS is suggested for the first time as a new analytical methodology for nicotine detection in real e-liquid samples. The use of Ag-SPEs reduces the analysis cost and electrochemistry allows the preparation of *in-situ* SERS substrates, avoiding the chemical synthesis of the nanostructures and the preparation of different substrates prior to the analysis. The proposed procedure avoids complex sample treatment or complex NPs synthesis, rendering this methodology a viable option for point of care analysis.

2. Material & methods / experimental

2.1. Chemicals and materials

Nicotine (99+ %, Sigma-Aldrich), lithium perchlorate (LiClO$_4$, 99+ %, reagent, ACROS Organics), potassium chloride (KCl, 99+ %, reagent, ACROS Organics), perchloric acid (HClO$_4$, 60 %, reagent, Panreac), sodium hydroxide (NaOH, 99+ %, reagent, ACROS Organics), hydrochloric acid (HCl, 37 %, reagent, COFARCAS) were analytical grade and used as received without further purification.

Aqueous solutions were freshly prepared using ultrapure water (18.2 MΩ cm resistivity at 25 °C, 2 ppb TOC, Milli-Q Direct 8, Millipore).

2.2. E-liquid samples

Twelve e-cigarette liquids advertised as pure nicotine, nicotine salts or nicotine-free with different flavours were purchased as test samples on a commercial website. Further details may be found in Table S1.

2.3. Instrumentation

TR-EC-SERS measurements were conducted using a customized SPELEC RAMAN (Metrohm-DropSens), with a 785 nm laser source operating at a power of 105 mW (335 W cm^{-2}) throughout the experiments. DropView SPELEC (Metrohm-DropSens) was the software used to acquire the spectroelectrochemical data. A different Ag-SPE (DRP-C013, Metrohm-DropSens) was utilised in each TR-EC-SERS experiment. The Ag-SPEs are composed of three electrodes: a working electrode (WE), a pseudo-reference electrode (RE), both of which are made of silver, and a carbon counter electrode (CE).

2.4. Spectroelectrochemistry measurements

Cyclic voltammetry (CV) was selected as the electrochemical technique for the TR-EC-SERS experiments. If not stated otherwise, the vertex potentials were +0.20 V and −0.20 V, starting at +0.20 V in the cathodic direction after an equilibration time of 5 s at the starting potential (Fig. S1). The scan rate was 0.02 Vs^{-1} in all experiments and, in all cases, two cycles were registered. All potentials are referenced to a silver pseudo-RE. The acquisition time of the Raman spectra was 1 s throughout this work.

Unless otherwise stated, all experiments were performed directly on Ag-SPEs with a pre-treatment step previous to the measurement step under the same electrochemical conditions as indicated above (Fig. S1). Subsequent to the pre-treatment step, the SPE was thoroughly washed with deionised water before the measurement step.

2.5. Scanning electron microscope images

A Zeiss GeminiSEM560 field-emission scanning electron microscope (FE-SEM) was used to obtain SEM images of the WE surface in its different states. An electron beam of 2 kV was used, with an in-lens secondary electrons detector.

2.6. Sample preparation

All samples (nicotine and e-liquids) were diluted in an appropriate medium used as electrolyte and in different concentrations of KCl as a precipitating agent.

2.7. PARAFAC analysis

Matlab R2024b was used to carry out PARAFAC analysis, using the N-way toolbox developed by Rasmus Bro [29].

3. Results and discussion

3.1. TR-EC-SERS. Synthesis of SERS substrates

As previously stated, numerous studies have been conducted to determine the presence of nicotine using SERS [16–22]. In most of the previous works, the synthesis of NPs by chemical processes and the subsequent preparation of the SERS substrates was carried out prior to SERS measurements. The use of expensive and labour-intensive synthesis techniques is often necessary, which introduces the additional challenge of the typical poor reproducibility of SERS substrates. In this study, TR-EC-SERS experiments have been used for the *in-situ* generation of silver nanoparticles (Ag-NPs) by oxidation–reduction cycles (ORC) of the WE, avoiding the costly processes mentioned above. Although it is not the first time that EC-SERS has been applied to the determination of nicotine [30], in this work, the SERS substrate is generated *in-situ* by ORC of the Ag-SPE surface in the presence of 0.1 M LiClO$_4$, 10 mM KCl and the corresponding volume of e-liquids. Thus, the presented methodology allows the direct measurement of diluted problem samples.

To ensure a good sensitivity and reproducibility of our measurements, a new protocol based on a pre-conditioning step has been developed. Fig. S1 outlines the electrochemical methodology employed to prepare the electrode and to acquire the data for nicotine analysis. Two main steps were undertaken to pre-condition the electrode and to quantify the target molecule. In the first step, the SPE was pre-conditioned using a 0.1 M LiClO$_4$ and 10 mM KCl electrolytic solution, applying +0.20 V for 5 s, and next carrying out two consecutive CVs from +0.20 V to −0.20 V at 0.02 Vs^{-1}. This pre-conditioning step is crucial for ensuring a better sensitivity and reproducibility of the experiments, as will be demonstrated in section 3.4. After thorough rinsing with deionized water, the SPE was immersed in the test solution containing nicotine and the electrolytic medium (0.1 M LiClO$_4$ and 10 mM KCl).

In the second step, Ag-NPs are generated and the Raman response of the analyte was concomitantly monitored in real time during the CV experiment. First a potential of +0.20 V was applied during 5 s, provoking the oxidation of the Ag^0 of the WE surface, generating high anodic currents in the first step of the experiment and resulting in the formation of AgCl, which precipitates on the WE surface in the form of nanocrystals [31]. Next, two potential scans were performed from +0.20 V to −0.20 V at 0.02 Vs^{-1}. Fig. 1A (blue line) shows the first potential cycle. A cathodic peak at −0.10 V is observed in the onward scan, related to the reduction of AgCl to Ag^0, with the subsequent
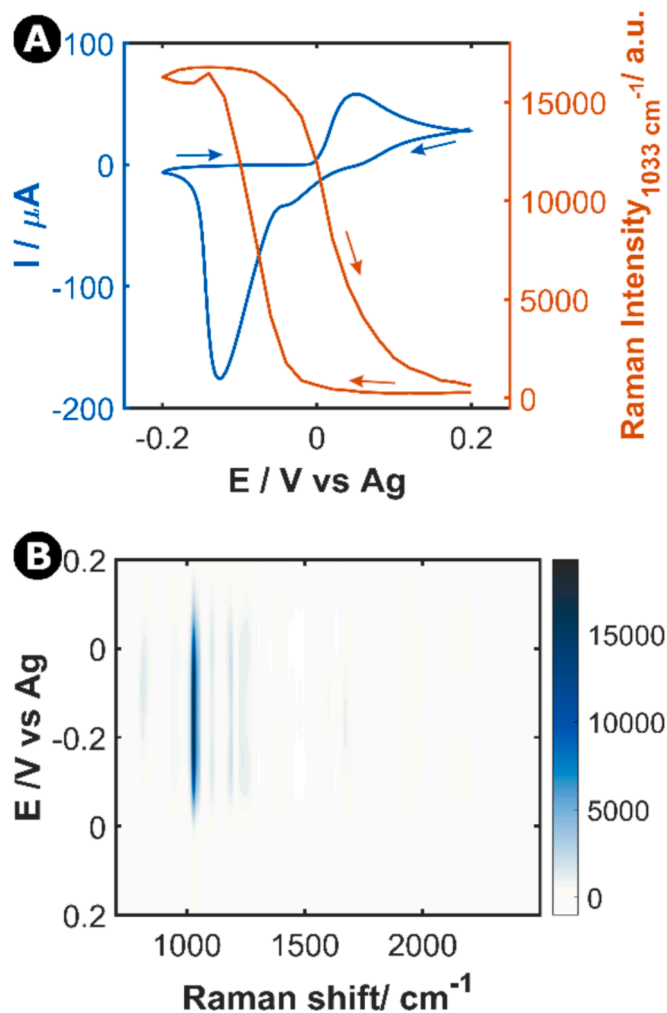
Fig. 1. (A) CV (blue line) and voltaRamangram (orange line) for a 1.5 µM nicotine sample in 0.1 M LiClO$_4$ and 10 mM KCl. The CV starts at +0.20 V in the cathodic direction down to the vertex potentials (−0.20 V) at a scan rate of 0.02 Vs^{-1}, before a pre-treatment at +0.20 V during 5 s. The voltaRamangram represents the evolution of the Raman intensity at 1033 cm^{-1}, the characteristic band of nicotine spectrum, versus the applied potential. (B) Contour plot with the evolution of the nicotine Raman spectra (between 700 and 2500 cm^{-1}) as a function of the applied potential during the first CV. (For interpretation of the references to colour in this figure legend, the reader is referred to the web version of this article.)

generation of Ag-NPs that are deposited on the WE surface [23]. In the backward scan, an anodic peak at +0.05 V is observed, which indicates the oxidation of Ag^0 to AgCl.

During this experiment, the Raman spectra of the electrode surface were studied. Fig. 1B depicts a surface plot with the evolution of the Raman spectra with the applied potential in the fingerprint region between 700 and 2500 cm^{-1}. As can be observed, the spectrum of nicotine exhibits a principal Raman band at 1033 cm^{-1}. Fig. 1A also shows the evolution of the characteristic Raman band of nicotine [30] at 1033 cm^{-1} (orange line) respect to the applied potential in the first potential cycle; this representation is known as voltaRamangram [23]. As can be observed, the Raman signal increases during the generation of Ag-NPs, reaching a stable maximum at the cathodic vertex potential, indicative of the SERS properties of the modified WE surface. Furthermore, a decrease in the Raman signal is observed during the backward scan when Ag-NPs become oxidised to form AgCl.

3.2. WE surface characterization

To gain a deeper insight into the structures formed during the experiment and their role in the observed SERS effect, the electrode surface was examined using SEM at specific potentials corresponding to key points in the aforementioned CV. The potentials at which SEM samples were acquired are numbered consecutively in Fig. S1. SEM images are presented in Fig. 2 and Fig. S2.

The first SEM images were taken from a pristine Ag-SPE (Figs. S2A, B). A planar surface is observed on the unmodified commercial Ag-SPE, free from any visible nanostructure on the Ag surface. Next, a set of images was taken once the pre-treatment protocol of an SPE was completed (Figs. S2C, D). Semi-cubic AgCl nanocrystals uniformly deposited on the electrode surface were observed at this point, in agreement with the results obtained in previous studies [31].

As shown in Fig. S1, the third sample was obtained in the measurement step, at the end of the 5 s equilibrium period at +0.20 V in which the Ag-SPE is oxidized before starting the CV for the measurement of nicotine. As illustrated in Fig. 2A and 2B, semi-cubic AgCl nanocrystals are homogeneously deposited covering the electrode surface [31]. Finally, Fig. 2C and 2D were obtained during the first potential cycle in the CV at a potential of −0.20 V, when the previously formed nanocrystals were reduced from AgCl to Ag^0, creating a homogeneous deposit of Ag-NPs on the WE surface. Therefore, the Raman enhancement is attributed to the presence of these nanostructures [23], which exhibit a maximum Raman signal when the surface is homogeneously covered with Ag-NPs, yielding a stable Raman response until the surface undergoes oxidation.

3.3. Raman bands assignment

Prior to nicotine quantification, the Raman characterization of the molecule under study was undertaken. The Raman spectrum of the pure nicotine molecule was compared with the SERS spectrum of the molecule in 0.1 M LiClO$_4$ and 10 mM KCl solution in the first potential cycle in the measurement step at a potential of −0.20 V. The Raman spectrum of the pure nicotine sample was measured from the pure chemical in its liquid state, while the SERS spectrum was obtained during a TR-EC-SERS experiment following the electrochemical protocol described in section 2.4. The Raman bands assignment of the nicotine spectrum is presented in Table S2 [30]. The two spectra display a highly remarkable degree of similarity, with only minor discrepancies evident, as illustrated in Fig. 3. The most characteristic band of nicotine due to the symmetric ring breathing of pyridine group is observed in both spectra, peaking at 1026 cm^{-1} in the pure Raman spectrum and at 1033 cm^{-1} in the SERS spectrum. These subtle variations in the spectra could be attributed to the interaction of the nicotine with the electrolytic medium and/or with the surface of the SERS substrate.

3.4. SEC optimization for nicotine quantification

One of the key advantages of TR-EC-SERS experiments lies in their ability to meticulously control experimental parameters, thereby enabling precise manipulation of the SERS substrate properties. These parameters include the electrochemical technique, the electrolyte composition, and the precipitating agents. Minor alterations of these parameters result in the formation of different nanostructured surfaces, which exhibit variations in shape, size, and density of NPs on the WE surface [26,32]. Additionally, the overall surface charge may modulate their interfacial interaction with specific analytes, including physisorption and chemisorption [26,33], allowing to modulate the analyte/substrate interaction.

In this context, several key parameters in our experimental protocol, such us the electrolyte, KCl concentration and the pre-treatment of the SPE, were investigated and optimised for the detection of nicotine.

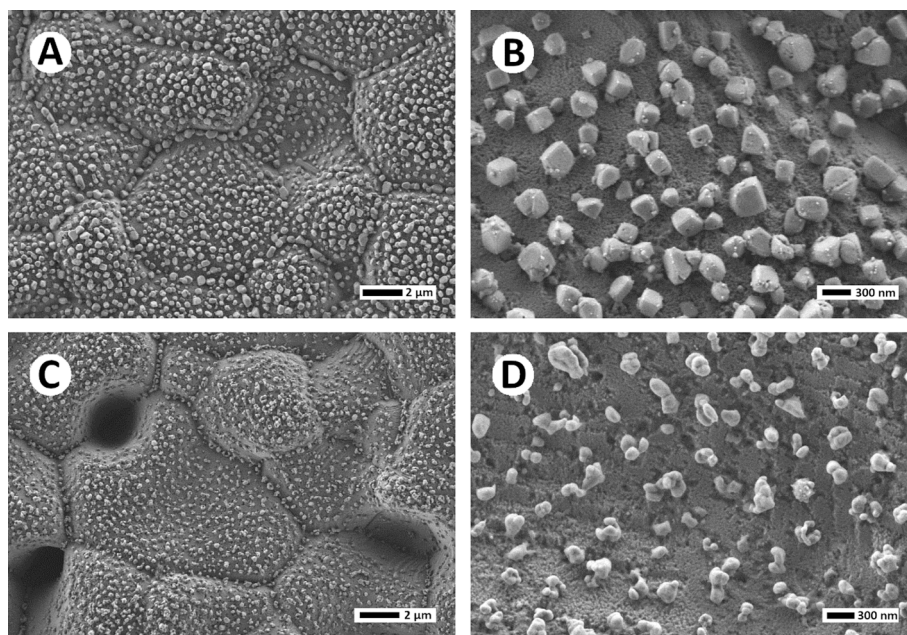Previous studies on this topic demonstrates that the electrolytic

Fig. 2. SEM images of the Ag-SPEs surface during the measurement step in a SEC experiment. (A, B) SEM images at different scales of the Ag-SPE surface taken after the equilibrium time at +0.20 V applied for 5 s. (C, D) SEM images at different scales of the Ag-SPE surface taken at −0.20 V during the first potential cycle.
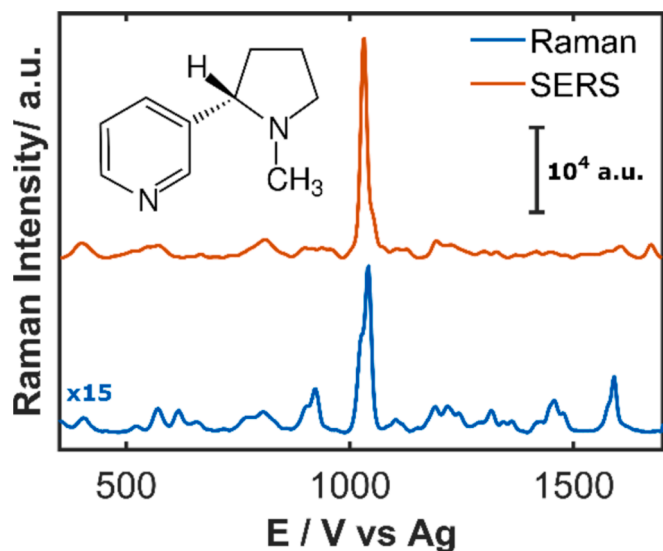

Fig. 3. Raman spectrum of nicotine in its pure state (blue) and SERS spectrum of 10 μM nicotine at −0.20 V in 0.1 M LiClO$_4$ and 10 mM KCl medium. For better comparison, the Raman spectrum (blue) of the pure nicotine has been scaled up by a factor of 15. The molecular structure of the compound has been included as inset. (For interpretation of the references to colour in this figure legend, the reader is referred to the web version of this article.)

medium greatly influences the EC-SERS response of a variety of analytes [25,26,30,33]. Therefore, we studied the evolution of nicotine signal in four different media: KCl/NaOH, KCl/HCl, KCl/LiClO$_4$ and KCl/HClO$_4$. Whereas the concentrations of nicotine and KCl were kept constant, the vertex potentials were adjusted in each case to achieve surface oxidation/reduction suitable for generating nanostructured surfaces. The results of this study are summarized in Fig. S3. The enhancement of the Raman signal was observed for all the studied electrolytic media, with a maximum enhancement observed when using LiClO$_4$ (Fig. S3D). Therefore, these conditions were selected as the supporting electrolyte for the subsequent experiments.

KCl was chosen as precipitant due to its extensive use in this type of methodology [23,30,31,34]. In addition, the Raman enhancement of nicotine was monitored as a function of KCl concentration, between 1 and 50 mM (Fig. S4). As was expected, a generalized increase of the electrochemical current during the CV at high KCl concentration (Fig. S4A) was observed. It might be commonly assumed that increasing the surface roughness would boost the Raman signal. However, as is demonstrated in Fig. S4B, the concentration of the precipitating agent that produces the greatest Raman enhancement is 10 mM KCl. These results suggest that low concentrations of the precipitating agent yield a low number of electrochemically generated Ag-NPs, resulting in a slight amplification of the Raman signal. Furthermore, at elevated concentrations of the precipitating agent, the size of the generated Ag-NPs could not be optimal for the amplification of the Raman signal.

One of the main drawbacks of SERS is an intrinsic lack of reproducibility for some substrates. Therefore, the development of strategies to improve the overall reproducibility is fundamental to use this technique in chemical analysis. From the different strategies studied, the application of a pre-conditioning step of the Ag-SPE by electrodepositing AgCl nanostructures provides the best results. Fig. S5 compares the results obtained from direct measurements on the electrode without pre-treatment of the WE (Fig. S5A) and those obtained after the pre-treatment step (Fig. S5B). As can be seen, the evolution of the Raman signal of nicotine with the potential is similar in the two cases. However, the pre-treatment step of the Ag-SPE with two additional ORC provides greater enhancement of the Raman signal (10000 counts *vs* 6000 counts) and better %RSD values (2.1 % vs 6.5 % for n = 3).

3.5. Quantitative analysis

Following the optimized protocol described above, the linear character of the EC-SERS signal was evaluated with six standard samples of nicotine (100–1500 nM), each one replicated three times. Fig. 4A shows the voltaRamangrams at 1033 cm^{-1} for the different nicotine concentrations during the first potential cycle of the measurement step (Fig. S1). The Raman signal at the characteristic band of nicotine (1033 cm^{-1}) registered at the vertex potential, −0.20 V, was chosen as the optimal point to perform the calibration curve shown in Fig. 4B.

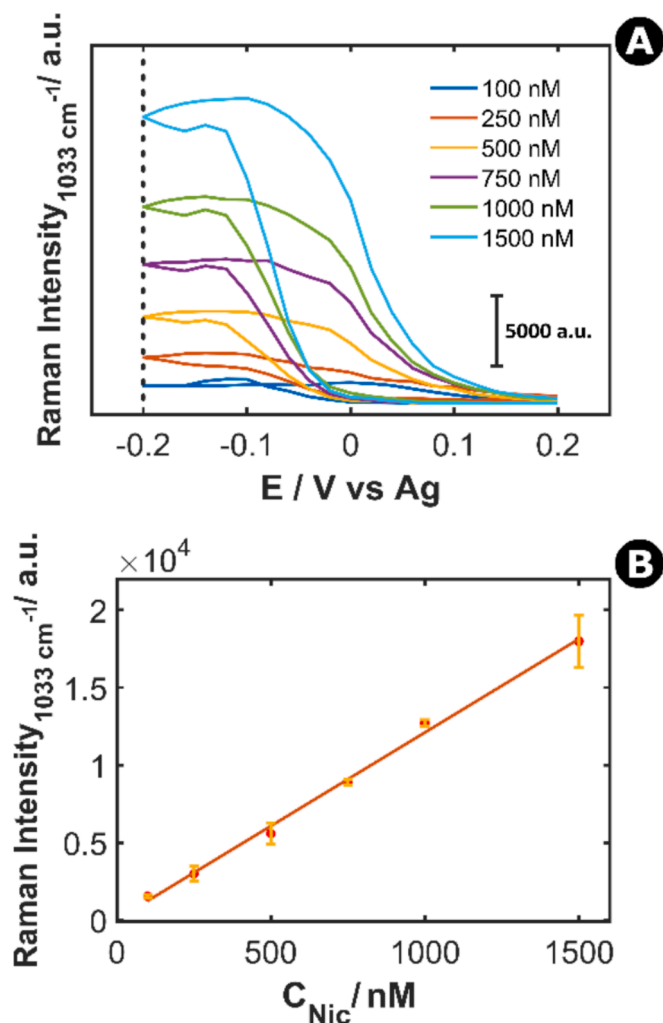The calibration curve (Fig. 4B) shows a very good correlation in the

Fig. 4. (A) VoltaRamangrams at 1033 cm^{-1} at different concentrations of nicotine (100, 250, 500, 750, 1000 and 1500 nM) in presence of 0.1 M LiClO$_4$ and 10 mM KCl, during the first potential cycle of the measurement step. (B) Calibration curve for nicotine measured at 1033 cm^{-1} at the cathodic vertex potential, −0.20 V.

studied concentration range, resulting in the good analytical figures of merit given in Table 1. The regression curve demonstrates excellent linearity and repeatability of the slope for the EC-SERS measurements. The limit of detection (LOD) was calculated using the accepted IUPAC recommendations based on types I and II errors (false positives and false negatives) [35]. A value of 185 nM for the LOD was obtained, demonstrating the high sensitivity of EC-SERS. Taking into account that the range of nicotine concentration in e-liquids falls within 6 and 111 mM [20], the new analytical approach should to be useful to determine nicotine in this challenging sample matrices. This methodology enables the capacity to operate at low dilutions, which is really helpful to minimize the influence of the interfering components of e-liquids.

The presented results demonstrate that this TR-EC-SERS method is reliable, repeatable, and sensitive. Using this analytical protocol, nicotine was determined on a batch of test samples, which included e-liquids with different nicotine concentrations (see Table S1). The e-liquids samples were pre-treated following the procedure outlined in section 2.6. The resulting data are presented in Table 2.

As can be seen in Table 2, the concentration of nicotine estimated for complex problem samples (e-liquid) are very close to the concentration value labelled for each sample. An statistical approach is conducted to demonstrate that the recovery values obtained exhibit concordance with the results of the linear regression (Fig. S6) [36]. The values of nicotine concentrations indicated on the packaging of the e-liquids were plotted against the nicotine concentrations predicted by the linear regression model, resulting in a significant value of 1 for the slope (0.9921) and a significant value of 0 for the intercept (−0.5548), obtaining the following confidence intervals at 95 % of confidence for the slope and intercept, [0.88, 1.10] and [-1.65, 0.54], respectively. Good values of dispersion of the results and recoveries were obtained considering the nature of the technique employed [37]. These values demonstrate the good performance of the EC-SERS method based on the oxidation/reduction of a Ag-SPE in a 10 mM KCl and 0.1 M LiClO$_4$ medium for the determination of nicotine.

However, the predicted values for samples 2 and 10 appear do not follow the general trend observed in the other samples, exhibiting a clear discrepancy between the nicotine concentration reported in the label and the value predicted by our method. This discrepancy also affects the recovery values, which deviate significantly from the average recovery value of the remaining samples (with the exception of samples 2 and 10, with low nicotine concentration, and samples 3 and 5, without nicotine according the supplier, the average recovery value is 101 %).

These results have been analysed using a univariate regression model of the experimental EC-SERS data. Although the model obtained is a valuable tool for estimating nicotine concentrations in complex samples, it is challenging to understand why the samples 2 and 10 can interfere in our method without additional information. For this reason, we used multivariate analysis to obtain more information about these outliers.

3.6. Multivariate analysis

One of the most significant attributes of TR-EC-SERS is the trilinear nature of its data. In these experiments, the Raman signal depends on three different and independent variables which are obtained simultaneously: Raman shifts, time or potential applied, and analyte concentration [23]. The TR-EC-SERS feature enables the generation of a three-way array data that can be analysed using different multivariate statistical tools.

To obtain more information about the e-liquids number 2 and 10 and why they cannot be determined using the detection method proposed, Parallel Factor Analysis (PARAFAC) [38] was used to analyse the trilinear data. PARAFAC is a multivariate statistical tool that is employed to analyse the three-way array of Raman data without

Table 1
Analytical figures of merit for the linear regression model obtained at the Raman shift 1033 cm^{-1} and −0.20 V in the backward scan during TR-EC-SERS experiments.

Slope (nM^{-1})	Intercept (a.u.)	R^2	S$_{yx}$	LOD (nM)	Repeatability (%)
12.06	12.96	0.996	436.74	185	7.91

Table 2
Information of e-liquids examined in this study.

Sample N°	Labelled nicotine level (mg/mL)	Nicotine determined (mg/mL)	Confidence interval (mg/mL)	Recovery (%)
1	18	16.11	16.11 ± 3.94	89.52
2	3	1.85	1.85 ± 0.14	61.56
3	0	0.08	0.08 ± 0.01	na
4	6	5.73	5.73 ± 0.75	95.50
5	0	0.06	0.06 ± 0.01	na
6	12	9.90	9.90 ± 1.22	82.46
7	20	21.20	21.20 ± 3.60	106.03
8	6	4.69	4.69 ± 0.56	78.19
9	12	11.51	11.51 ± 1.26	95.96
10	3	2.10	2.10 ± 0.32	69.88
11	6	5.98	5.98 ± 0.11	99.63

na = not applicable.

providing any additional information required about the system o process measured. This statistical tool is used to construct the mathematical model capable of identifying the factors that most influence the Raman spectroscopic response [23,39,40].

The matrix dimension of the three-way array of Raman data is defined by the Raman intensity values between 720 and 1800 cm^{-1}, during the first potential cycle in the measurement step, for all the experiments performed in the calibration model and the 11 e-liquid samples analysed.

The number of components for the PARAFAC model was selected based on a study of the variation of the corcondia (core consistency diagnostic) and the PARAFAC residual fit. As can be observed in Fig. S7, the different PARAFAC residual fit values decrease to stabilise from 3 components onwards, whereas the optimal corcondia values are significant when 1 to 3 components are selected for the PARAFAC model. Therefore, PARAFAC analysis was carried out selecting three components, obtaining a corcondia value of 97.70 %, indicating that the model is appropriate and reliable [41].

The first component (component A, Fig. 5A, blue line) is linked with the nicotine concentration, as can be deduced from the similar shape of the loadings plot versus Raman shift of this component with respect to the nicotine spectrum (Fig. S8B). The second component (component B,
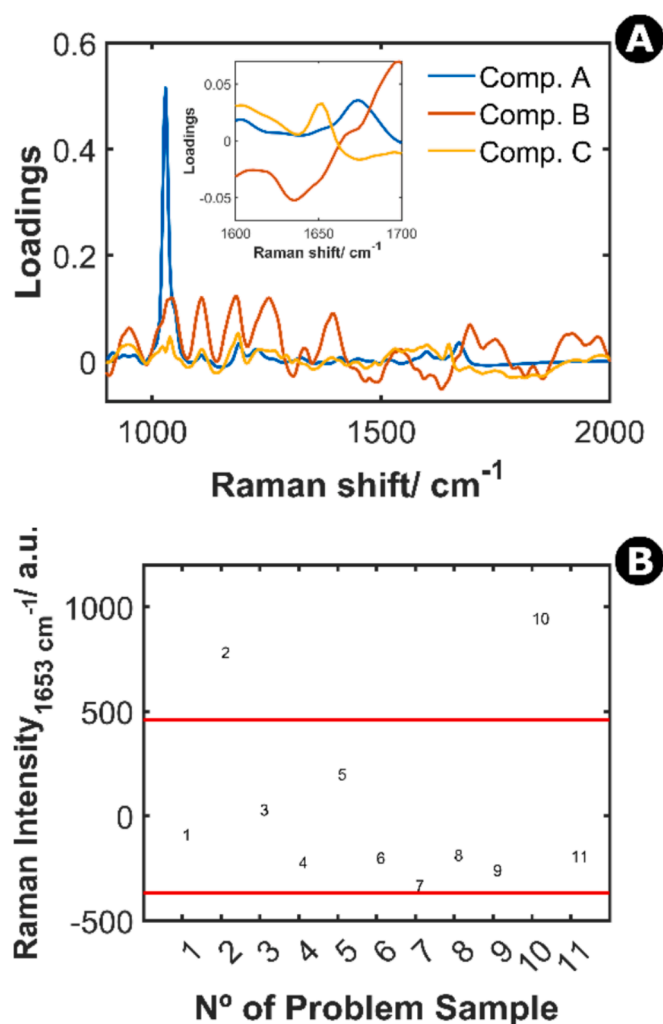

Fig. 5A, orange line) is related to some changes in the background signal, which is clearly affecting the measurements. The third component (component C, Fig. 5A, yellow line) is related to the presence in the e-liquid samples of some compound different to nicotine. These components were easily identified, since the data given to the PARAFAC model were data corrected with a baseline.

When the loadings of the three PARAFAC components are plotted versus the applied potential, the line shape of component A (Fig. S8C, blue line) is similar to the voltaRamangram of nicotine (Fig. S8C, green line). The evolution of loadings related to component B along the applied potential (Fig. S8A, orange line) can be related to change in the background signal. Finally, the presence of an unidentified contaminant is noted in component C (Fig. S8A, yellow line), exhibiting a noticeable correlation with the applied potential (corresponding to a voltaRamangram of an unknown interfering compound), but clearly different to the behaviour of component A ascribed to nicotine.

As was demonstrated in the previous section, samples 2 and 10 are affected by an unknown factor that affects the proposed analytical method. These results suggest that an unidentified compound is present in these outlier samples, which interferes clearly in the EC-SERS response of nicotine. After PARAFAC multivariate analysis with three factors is conducted, the third component should be related with another compound different from nicotine, which could be a nicotine derivate product because it contributes also to the 1033 cm^{-1} peak, affected by the SERS effect (Fig. 5A and Fig. S8A, yellow line). Upon a closer examination of data corresponding to samples 2 and 10, it can be observed that these samples exhibit a small and characteristic spectral feature close to 1653 cm^{-1}, also observed in the plot of the loadings of component C respect to the Raman shift between 1600 and 1700 cm^{-1} (Inset Fig. 5A, yellow line). To confirm this hypothesis, the Raman intensity at 1653 cm^{-1} at 0.00 V in the backward scan is represented respect to the sample number (Fig. 5B). It has been selected the potential of 0.00 V because is the potential where the evolution of component C reaches a maximum (Fig. S8A, yellow line). As can be observed, most of samples exhibit Raman intensity value at 1653 cm^{-1} that is approximately zero. However, samples 2 and 10, show a clear different response at 1653 cm^{-1} and 0.00 V. A t-test was performed to confirm that samples 2 and 10 fall outside the test limits, represented in red lines in Fig. 5B, demonstrating that the deviation of the samples 2 and 10 is statistically significant. As can be seen in Fig. 5B, samples 2 and 10 are heavily influenced by this unknown compound which is interfering the measurement. Although the cause of this interference is unknown, the presented experimental methodology, coupled with multivariate statistical tools, is capable of identifying outlier samples, demonstrating the utility and versatility of TR-EC-SERS, which not only can be used for quantitative analysis but also for the detection of outlier samples. In this particular case, PARAFAC is an extraordinary tool to find out the reason for the low values obtained in samples 2 and 10, but unfortunately no improvement in the predictions of the concentration of nicotine is obtained, as can be observed in Table S3. As the interfering compound is not identified, it is very difficult to train the mathematical model to be able of discriminate the weight of this compound in the global SERS signal. Although the results using PARAFAC with one component are slightly better than the univariate calibration, using only the univariate signal at 1033 cm^{-1} makes simplest the analysis of this type of samples. Surprisingly, no improvement in the prediction was observed using the PARAFAC model which identifies the interfering compound. Our main hypothesis is that the interfering compound is a nicotine related product which cannot be easily resolved with the PARAFAC model. This fact could also explain that PARAFAC with only one component explains slightly better the recoveries. In consideration of our analytical methodology, it is imperative to direct particular attention to this region of the spectrum, as samples displaying a signal at 1653 cm^{-1} do not provide a perfect accuracy, although good results were obtained.

Fig. 5. (A). Loadings of each component versus Raman shift after PARAFAC analysis. Additionally, an inset is provided, featuring a closer examination of the image, centred within the range of 1600 to 1700 cm^{-1}. (B) Raman intensity at 1653 cm^{-1} at a potential of 0.00 V in the backward scan for the 11 different e-liquid samples.

4. Conclusions

A new analytical protocol based on time-resolved EC-SERS has been developed for the determination of nicotine. The reproducibility of this protocol has been improved by performing an electrochemical pre-treatment of the Ag-SPE in order to generate a homogenous distribution of AgCl semi-cubic nanocrystals which are the precursors of the Ag-NPs. SEM images demonstrate that a uniform layer of Ag-NPS are generated on the electrode surface. The Ag-NPs enhanced the Raman signal of nicotine, allowing the detection of this compound at nanomolar level. The high sensitivity of the analytical method allows the quantitative analysis of diluted samples of e-liquids, helping to avoid any interfering compound present in these complex samples. TR-EC-SERS can be used not only to determine nicotine but also to detect interfering compounds by using PARAFAC. This multivariate tool allows the deconvolution of the Raman spectra without any additional information about the compounds present in the complex samples, showing a high potential to detect outliers.

CRediT authorship contribution statement

Luis Romay: Writing – review & editing, Writing – original draft, Visualization, Validation, Methodology, Investigation, Formal analysis, Data curation, Conceptualization. **Martin Perez-Estebanez:** Writing – review & editing, Visualization, Conceptualization. **Aranzazu Heras:** Writing – original draft, Resources, Project administration, Funding acquisition, Formal analysis. **Alvaro Colina:** Writing – review & editing, Writing – original draft, Validation, Supervision, Resources, Project administration, Methodology, Investigation, Funding acquisition, Formal analysis, Data curation, Conceptualization.

Declaration of competing interest

The authors declare that they have no known competing financial interests or personal relationships that could have appeared to influence the work reported in this paper.

Acknowledgments

Appendix A. Supplementary data

Supplementary data to this article can be found online at https://doi.org/10.1016/j.microc.2024.112551.

Data availability

Data will be made available at the repository of the Universidad de Burgos

References

[1] R. Grana, N. Benowitz, S.A. Glantz, E-cigarettes: a scientific review, Circulation 129 (2014) 1972–1986, https://doi.org/10.1161/CIRCULATIONAHA.114.007667.

[2] C. Franck, K.B. Filion, J. Kimmelman, R. Grad, M.J. Eisenberg, Ethical considerations of e-cigarette use for tobacco harm reduction, Respir. Res. 17 (2016) 53, https://doi.org/10.1186/s12931-016-0370-3.

[3] A.R. Romberg, E.J. Miller Lo, A.F. Cuccia, J.G. Willett, H. Xiao, E.C. Hair, D.M. Vallone, K. Marynak, B.A. King, Patterns of nicotine concentrations in electronic cigarettes sold in the United States, 2013-2018, Drug Alcohol Depend. 203 (2019) 1–7. 10.1016/j.drugalcdep.2019.05.029.

[4] B. Davis, M. Dang, J. Kim, P. Talbot, Nicotine Concentrations in Electronic Cigarette Refill and Do-It-Yourself Fluids, Nicotine Tob. Res. 17 (2015) 134–141, https://doi.org/10.1093/ntr/ntu080.

[5] D. Ramamurthi, P.A. Gall, N. Ayoub, R.K. Jackler, Leading-Brand Advertisement of Quitting Smoking Benefits for E-Cigarettes, Am. J. Public Health 106 (2016) 2057–2063, https://doi.org/10.2105/AJPH.2016.303437.

[6] G. St, D.L.E. Helen, Public Health Consequences of e-Cigarette Use, JAMA, Intern. Med. 178 (2018) 984–986, https://doi.org/10.1001/jamainternmed.2018.1600.

[7] D.R. Miller, K. Buettner-Schmidt, M. Orr, K. Rykal, E. Niewojna, A systematic review of refillable e-liquid nicotine content accuracy, J. Am. Pharm. Assoc. 61 (2021) 20–26, https://doi.org/10.1016/j.japh.2020.09.006.

[8] B. Mayer, How much nicotine kills a human? Tracing back the generally accepted lethal dose to dubious self-experiments in the nineteenth century, Arch. Toxicol. 88 (2014) 5–7, https://doi.org/10.1007/s00204-013-1127-0.

[9] A. Taylor, K. Dunn, S. Turfus, A review of nicotine-containing electronic cigarettes—Trends in use, effects, contents, labelling accuracy and detection methods, Drug Test. Anal. 13 (2021) 242–260, https://doi.org/10.1002/dta.2998.

[10] A.M. Harvanko, C.M. Havel, P. Jacob, N.L. Benowitz, Characterization of Nicotine Salts in 23 Electronic Cigarette Refill Liquids, Nicotine Tob. Res. 22 (2020) 1239–1243, https://doi.org/10.1093/ntr/ntz232.

[11] J. Etter, E. Zäther, S. Svensson, Analysis of refill liquids for electronic cigarettes, Addiction 108 (2013) 1671–1679, https://doi.org/10.1111/add.12235.

[12] M. Famele, J. Palmisani, C. Ferranti, C. Abenavoli, L. Palleschi, R. Mancinelli, R. M. Fidente, G. de Gennaro, R. Draisci, Liquid chromatography with tandem mass spectrometry method for the determination of nicotine and minor tobacco alkaloids in electronic cigarette refill liquids and second-hand generated aerosol, J. Sep. Sci. 40 (2017) 1049–1056, https://doi.org/10.1002/jssc.201601076.

[13] M. Famele, C. Ferranti, C. Abenavoli, L. Palleschi, R. Mancinelli, R. Draisci, The Chemical Components of Electronic Cigarette Cartridges and Refill Fluids: Review of Analytical Methods, Nicotine Tob. Res. 17 (2015) 271–279, https://doi.org/10.1093/ntr/ntu197.

[14] B. Sharma, R.R. Frontiera, A.-I. Henry, E. Ringe, R.P. Van Duyne, SERS: Materials, applications, and the future, Mater. Today 15 (2012) 16–25, https://doi.org/10.1016/S1369-7021(12)70017-2.

[15] D. Cialla, A. März, R. Böhme, F. Theil, K. Weber, M. Schmitt, J. Popp, Surface-enhanced Raman spectroscopy (SERS): progress and trends, Anal. Bioanal. Chem. 403 (2012) 27–54, https://doi.org/10.1007/s00216-011-5631-x.

[16] Y. Chen, Y. Tang, P. Li, Y. Wang, Y. Zhuang, S. Sun, D. Wang, W. Wei, A core-molecule-shell Au@PATP@Ag nanorod for nicotine detection based on surface-enhanced Raman scattering technology, Anal. Chim. Acta 1278 (2023) 341739, https://doi.org/10.1016/j.aca.2023.341739.

[17] S.E.J. Bell, N.M.S. Sirimuthu, Rapid, quantitative analysis of ppm/ppb nicotine using surface-enhanced Raman scattering from polymer-encapsulated Ag nanoparticles (gel-colls), Analyst 129 (2004) 1032–1036, https://doi.org/10.1039/b408775e.

[18] O. Alharbi, Y. Xu, R. Goodacre, Simultaneous multiplexed quantification of nicotine and its metabolites using surface enhanced Raman scattering, Analyst 139 (2014) 4820–4827, https://doi.org/10.1039/C4AN00879K.

[19] N. Itoh, S.E.J. Bell, High dilution surface-enhanced Raman spectroscopy for rapid determination of nicotine in e-liquids for electronic cigarettes, Analyst 142 (2017) 994–998, https://doi.org/10.1039/C6AN02286C.

[20] J.-Y. Chien, Y.-C. Gu, H.-M. Tsai, C.-H. Liu, C.-Y. Yen, Y.-L. Wang, J.-K. Wang, C.-H. Lin, Rapid identification of nicotine in electronic cigarette liquids based on surface-enhanced Raman scattering, J. Food Drug Anal. 28 (2020) 302–308. 10.38212/2224-6614.1064.

[21] J.-Y. Chien, Y.-C. Gu, C.-H. Liu, H.-M. Tsai, C.-N. Lee, A.C. Yang, J. Huang, Y.-L. Wang, J.-K. Wang, C.-H. Lin, Rapid detection of nicotine and benzoic acid in e-liquids with surface-enhanced Raman scattering and artificial intelligence-assisted spectrum interpretation, J. Pharm. Biomed. Anal. 233 (2023) 115456, https://doi.org/10.1016/j.jpba.2023.115456.

[22] M.B. Mamián-López, R.J. Poppi, Standard addition method applied to the urinary quantification of nicotine in the presence of cotinine and anabasine using surface enhanced Raman spectroscopy and multivariate curve resolution, Anal. Chim. Acta 760 (2013) 53–59, https://doi.org/10.1016/j.aca.2012.11.023.

[23] C.L. Brosseau, A. Colina, J.V. Perales-Rondon, A.J. Wilson, P.B. Joshi, B. Ren, X. Wang, Electrochemical surface-enhanced Raman spectroscopy, Nat. Rev. Methods Prim. 3 (2023) 79, https://doi.org/10.1038/s43586-023-00263-6.

[24] S. Hernandez, L. Garcia, M. Perez-Estebanez, W. Cheuquepan, A. Heras, A. Colina, Multiamperometric-SERS detection of melamine on gold screen-printed electrodes, J. Electroanal. Chem. 918 (2022) 116478, https://doi.org/10.1016/j.jelechem.2022.116478.

[25] W. Cheuquepan, S. Hernandez, M. Perez-Estebanez, L. Romay, A. Heras, A. Colina, Electrochemical generation of surface enhanced Raman scattering substrates for the determination of folic acid, J. Electroanal. Chem. 896 (2021) 115288, https://doi.org/10.1016/j.jelechem.2021.115288.

[26] R. Moldovan, M. Perez-Estebanez, A. Heras, E. Bodoki, A. Colina, Activating the SERS features of screen-printed electrodes with thiocyanate for sensitive and robust EC-SERS analysis, Sensors Actuators B Chem. 407 (2024) 135468, https://doi.org/10.1016/j.snb.2024.135468.

[27] D. Martín-Yerga, A. Pérez-Junquera, M.B. González-García, J.V. Perales-Rondon, A. Heras, A. Colina, D. Hernández-Santos, P. Fanjul-Bolado, Quantitative Raman

spectroelectrochemistry using silver screen-printed electrodes, Electrochim. Acta 264 (2018) 183–190, https://doi.org/10.1016/j.electacta.2018.01.060.

[28] L. Romay, P. Nuñez-Marinero, J.V. Perales-Rondon, A. Heras, F.J. del Campo, A. Colina, New screen-printed electrodes for Raman spectroelectrochemistry. Determination of p-aminosalicylic acid, Anal. Chim. Acta 1325 (2024) 343095, https://doi.org/10.1016/j.aca.2024.343095.

[29] C.A. Andersson, R. Bro, The N-way Toolbox for MATLAB, Chemom. Intell. Lab. Syst. 52 (2000) 1–4, https://doi.org/10.1016/S0169-7439(00)00071-X.

[30] T.E. Barber, M.S. List, J.W. Haas, E.A. Wachter, Determination of Nicotine by Surface-Enhanced Raman Scattering (SERS), Appl. Spectrosc. 48 (1994) 1423–1427, https://doi.org/10.1366/0003702944027985.

[31] S. Hernandez, M. Perez-Estebanez, W. Cheuquepan, J.V. Perales-Rondon, A. Heras, A. Colina, Raman, UV–Vis Absorption, and Fluorescence Spectroelectrochemistry for Studying the Enhancement of the Raman Scattering Using Nanocrystals Activated by Metal Cations, Anal. Chem. 95 (2023) 16070–16078, https://doi.org/10.1021/acs.analchem.3c01172.

[32] D. Martín-Yerga, A. Pérez-Junquera, M.B. González-García, D. Hernández-Santos, P. Fanjul-Bolado, Towards single-molecule in situ electrochemical SERS detection with disposable substrates, Chem. Commun. 54 (2018) 5748–5751, https://doi.org/10.1039/C8CC02069H.

[33] N. Leopold, A. Stefancu, K. Herman, I.S. Tódor, S.D. Iancu, V. Moisoiu, L.F. Leopold, The role of adatoms in chloride-activated colloidal silver nanoparticles for surface-enhanced Raman scattering enhancement, Beilstein J. Nanotechnol. 9 (2018) 2236–2247, https://doi.org/10.3762/bjnano.9.208.

[34] C.E. Ott, M. Perez-Estebanez, S. Hernandez, K. Kelly, K.A. Dalzell, M.J. Arcos-Martinez, A. Heras, A. Colina, L.E. Arroyo, Forensic Identification of Fentanyl and its Analogs by Electrochemical-Surface Enhanced Raman Spectroscopy (EC-SERS) for the Screening of Seized Drugs of Abuse, Front. Anal. Sci. 2 (2022) 1–12, https://doi.org/10.3389/frans.2022.834820.

[35] A.C. Olivieri, Analytical Figures of Merit: From Univariate to Multiway Calibration, Chem. Rev. 114 (2014) 5358–5378, https://doi.org/10.1021/cr400455s.

[36] A.G. González, M.A. Herrador, A.G. Asuero, Intra-laboratory testing of method accuracy from recovery assays, Talanta 48 (1999) 729–736, https://doi.org/10.1016/S0039-9140(98)00271-9.

[37] J. Langer, D. Jimenez de Aberasturi, J. Aizpurua, R.A. Alvarez-Puebla, B. Auguié, J.J. Baumberg, G.C. Bazan, S.E.J. Bell, A. Boisen, A.G. Brolo, J. Choo, D. Cialla-May, V. Deckert, L. Fabris, K. Faulds, F.J. García de Abajo, R. Goodacre, D. Graham, A.J. Haes, C.L. Haynes, C. Huck, T. Itoh, M. Käll, J. Kneipp, N.A. Kotov, H. Kuang, E.C. Le Ru, H.K. Lee, J.-F. Li, X.Y. Ling, S.A. Maier, T. Mayerhöfer, M. Moskovits, K. Murakoshi, J.-M. Nam, S. Nie, Y. Ozaki, I. Pastoriza-Santos, J. Perez-Juste, J. Popp, A. Pucci, S. Reich, B. Ren, G.C. Schatz, T. Shegai, S. Schlücker, L.-L. Tay, K.G. Thomas, Z.-Q. Tian, R.P. Van Duyne, T. Vo-Dinh, Y. Wang, K.A. Willets, C. Xu, H. Xu, Y. Xu, Y.S. Yamamoto, B. Zhao, L.M. Liz-Marzán, Present and Future of Surface-Enhanced Raman Scattering, ACS Nano 14 (2020) 28–117, https://doi.org/10.1021/acsnano.9b04224.

[38] R. Bro, Parafac., Tutorial and applications, Chemom. Intell. Lab. Syst. 38 (1997) 149–171, https://doi.org/10.1016/S0169-7439(97)00032-4.

[39] J.V. Perales-Rondon, S. Hernandez, D. Martin-Yerga, P. Fanjul-Bolado, A. Heras, A. Colina, Electrochemical surface oxidation enhanced Raman scattering, Electrochim. Acta 282 (2018) 377–383, https://doi.org/10.1016/j.electacta.2018.06.079.

[40] S. Hernandez, J.V. Perales-Rondon, A. Heras, A. Colina, Determination of uric acid in synthetic urine by using electrochemical surface oxidation enhanced Raman scattering, Anal. Chim. Acta 1085 (2019) 61–67, https://doi.org/10.1016/j.aca.2019.07.057.

[41] R. Bro, H.A.L. Kiers, A new efficient method for determining the number of components in PARAFAC models, J. Chemom. 17 (2003) 274–286, https://doi.org/10.1002/cem.801.